

Supplementary Information

Nanoporous polymer particles made by suspension polymerization: spontaneous symmetry breaking in hydrogen bonded smectic liquid crystalline droplets and high adsorption characteristics

H. P. C. van Kuringen, D. J. Mulder, E. Beltran, D. J. Broer, A. P. H. J. Schenning

S1 Materials and Methods

Materials

The cross-linker, 4-((4-(6-(acryloyloxy)hexyloxy)phenoxy)carbonyl)phenyl 4-(6-(acryloyloxy)hexyloxy) benzoate (C6H) and the mono acrylates 4-(6-acryloxy-hexyl-1-oxy)benzoic acid (6OBA), 4-(5-acryloxy-pentyl-1-oxy)benzoic acid (5OBA) and 4-(3-acryloxy-propyl-1-oxy)benzoic acid (3OBA), were custom made by Synthron Chemicals, Germany. The photo initiator, Irgacure 907, and inhibitor, Irganox 1076, were supplied by Ciba Specialty Chemicals. Stabilizer polyvinylpyrrolidone (PVP) (Mw 29000) was purchased from Sigma Aldrich.

Procedure

The nOBA - C6H 90-10 contains 85.3 wt% of nOBA (6OBA : 5OBA : 3OBA in a 1:1:1 weight ratio) and 9.4 wt% C6H. 5 wt% Initiator and 0.25 wt% inhibitor were added. For the phase behavior and monomer droplet study no initiator was added and the LCs were mixed by dissolving in tetrahydrofuran which was subsequently evaporated. The continuous phase, consisting of 56 mL distilled water and 0.4 gram PVP was pre-heated at the nematic phase temperature and poured over the molten monomer mixture (4 grams). The temperature was set just above the smectic to nematic phase transition. These two liquids were homogenized with an IKA homogenizer (T25 digital Ultra-Turrax®) for 10 min at 4000 rpm. The stable emulsion was transferred to a pre-heated (40 °C) 100 mL round bottom flask equipped with a magnetic stirrer operating at 200 rpm. The polymerization was started once the temperature of the emulsion was stabilized at 40 °C. This was done by immersing a quartz rod acting as a waveguide which was connected to a UV light source (250 – 450 nm optical transmission filter) in the emulsion. Stirring and heating of the emulsion was maintained for 1 hour to complete the polymerization. The reaction mixture was cooled to room temperature and filtered through a 7 µm pore size nylon cloth. The filtrate was centrifuged to recover the particles, followed by an additional washing and centrifuge step. The particles were subsequently treated with 0.05 M KOH solution and again centrifuged.

Adsorption

The adsorption process was performed by using freshly prepared MB, or a mixture of MB and MO (Acros Organics) aqueous solutions.

Characterization

POM studies were conducted using a Leica CTR 6000 microscope equipped with two polarizers that were operated crossed with the sample in between, a Linkam hot-stage THMS600 with a Linkam TMS94 controller and a Leica DFC420 C camera. POM samples of the monomer mixture were prepared between an unrubbed poly imide (OPTMER AL 1051, JSR Corporation, Tokyo, Japan) coated glass plate and an uncoated cover glass. A DSC Q1000 from TA instruments was used with 10 °C / min temperature ramp ranging from -50 °C till 140 °C and 1 minute isotherm. The 1st heating and cooling cycle was used for characterization. XRD was performed on a Ganesha lab instrument equipped with a GeniX-Cu ultra-low divergence source producing X-ray photons with a wavelength of 1.54 Å and a flux of 1×10^8 ph/s. Scattering patterns were collected using a Pilatus 300K silicon pixel detector with 487×619 pixels of $172 \mu\text{m}^2$ in size. A glass capillary was filled with the particles or monomer mixture. The latter was heated till the isotropic phase was reached and subsequently cooled with 10 °C / min. FTIR spectra were obtained using a FTS 6000 Spectrometer from Bio-Rad equipped with Specac Golden gate diamond ATR and were signal-averaged over 50 scans at a resolution of 1 cm^{-1} . Varian Resolution Pro software was used for the analysis of the spectra. SEM characterisation was carried out on a Leo 1455VP SEM equipped with a 30 kV LaB6 filament with an Everhart-Thornley secondary electron detector and a Cambridge four quadrant backscatter detector. ImageJ software was used to determine particle size from the SEM and POM pictures. Dye absorbance measurements of solutions were performed in 1 cm path length quartz cells using an UV-VIS-NIR spectrophotometer (Shimadzu UV-3102).

S2 Characterization of monomer mixture

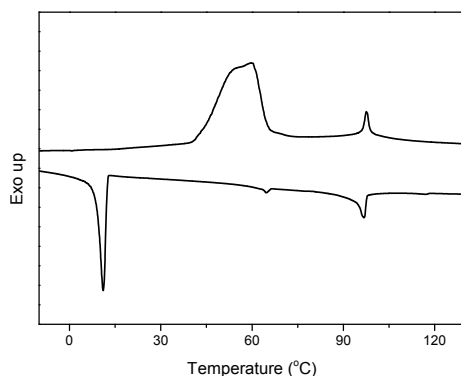


Fig. S1 DSC of the nOBA-C6H 90-10 monomer mixture. Upon heating a melting peak around 60 °C is observed followed by mesophase transitions. Upon cooling the monomer mixture exhibits a phase transitions at 97 °C, 65 °C and 10 °C.

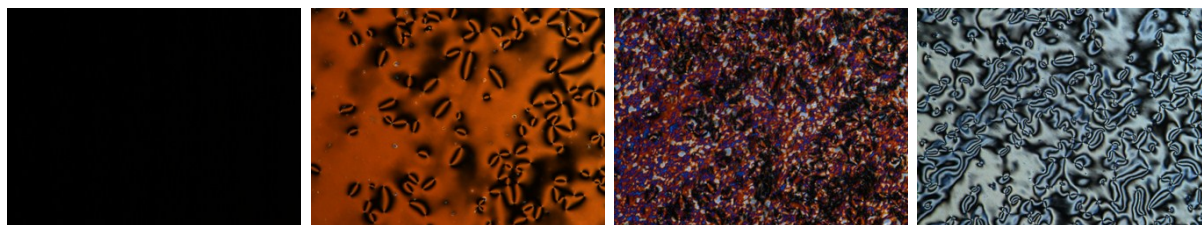


Fig. S2 POM pictures of the nOBA-C6H 90-10 monomer mixture. The mixture exhibits an isotropic phase above 97 °C. Between 97 °C and 65 °C a gradual transition from nematic to a skewed cybotactic nematic phase was observed. At 65 °C the mixture reached a smectic C phase which holds till below room temperature. From left to right: isotropic (102 °C), nematic (96 °C), skewed cybotactic nematic (88 °C) and smectic C (40 °C)

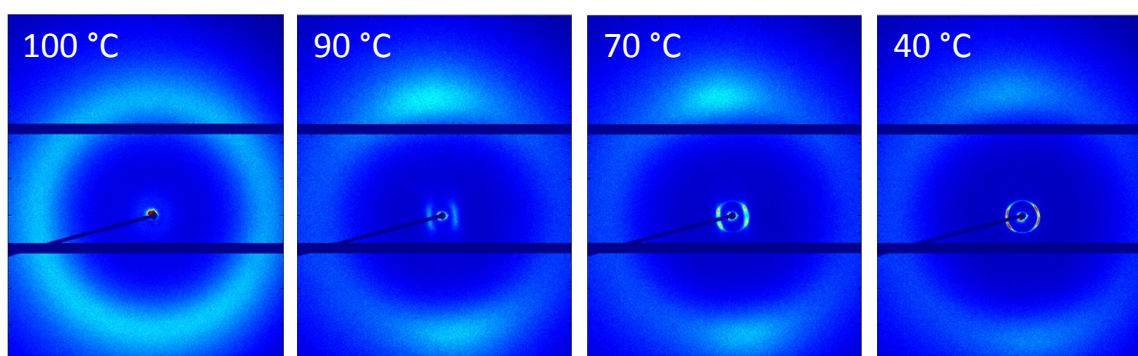


Fig. S3 XRD pictures of the nOBA-C6H 90-10 monomer mixture. From left to right: isotropic (100 °C), nematic (90 °C), skewed cybotactic nematic (70 °C) and smectic C (40 °C).

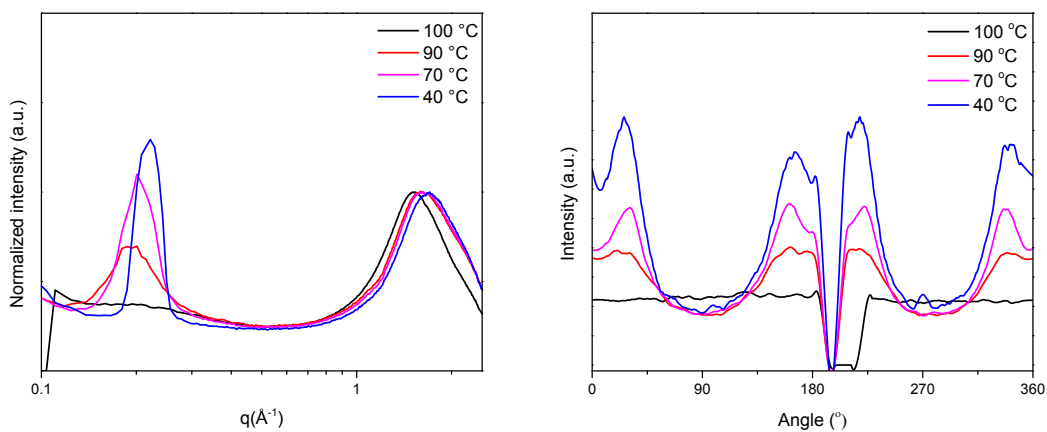


Fig. S4 Left: XRD 1D profiles of the pictures depicted in Fig. S3, showing the d-spacing signal at q : 0.18-0.26. Right: XRD 2θ profiles integrated over q : 0.18-0.26 showing the tilt angle of the skewed cybotactic nematic and smectic C phase. The tilt angle for the smectic C phase was temperature dependent and is 20° close to the nematic – smectic C transition and evolves to 30° close to room temperature, corresponding to an average molecular length of 3.3 nm.

S3 Characterization of monomer droplets

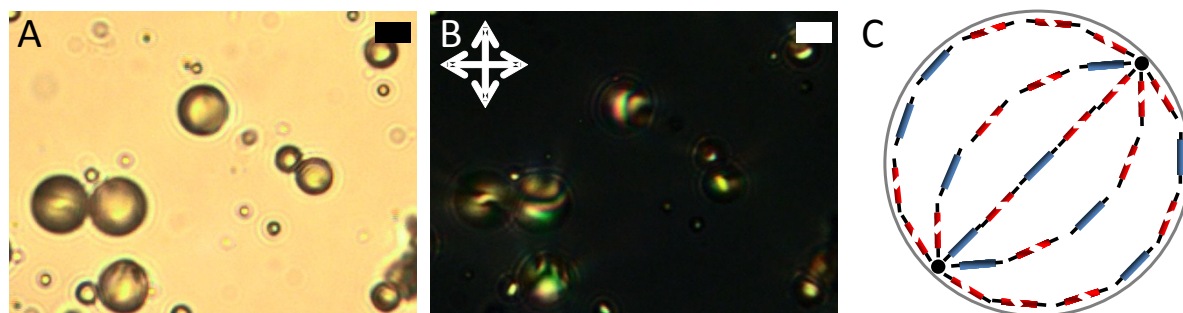


Fig. S5 Microscopy images of the of planar nematic LC droplets of the 90-10 mixture at 80 °C without (A) or with (B) crossed polarizers (crossed arrows). In those regions of a droplet where the projected orientation of the LC is uniform along the optical path, and either parallel or perpendicular to the polarizers, the LC appears to be dark. In the other regions of the droplet the LC appears bright. For visualization of the planar director profile some larger droplets are depicted. Scale bar is 10 μm . (C) Schematic drawing of possible director profile. The observation might point to a bipolar orientation, with planar orientation at the droplets surface. However, the molecular director might be tilted with respect the surface and the director (or its projection) at the surface might be twisted, deviating from the meridional lines.

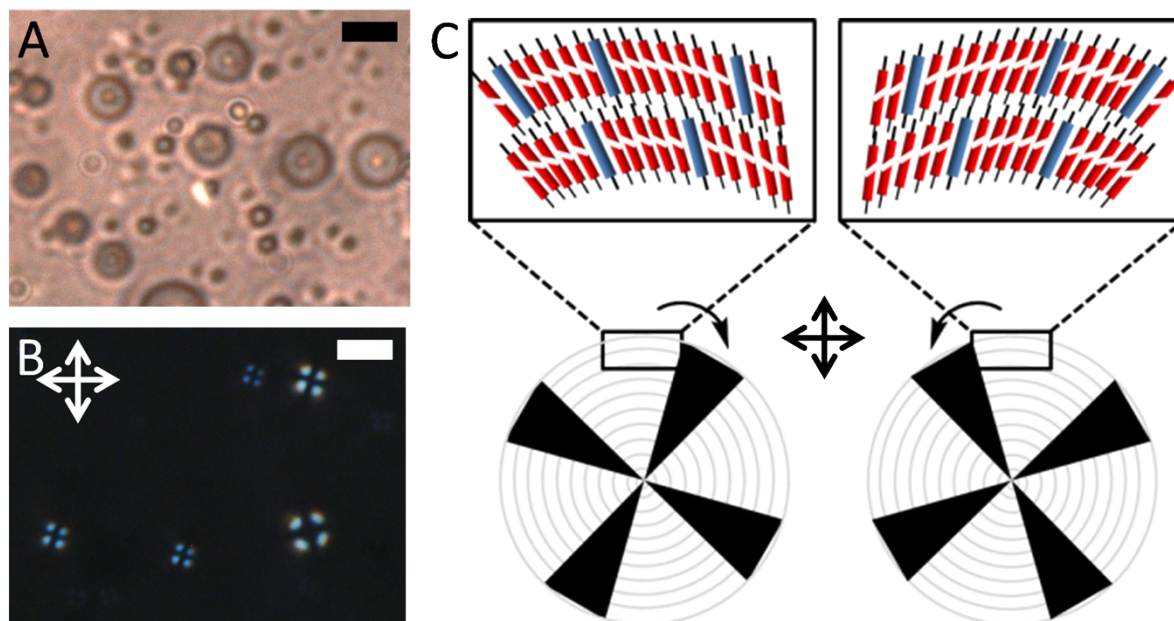


Fig. S6 Microscopy images and schematic drawings of the onion-like smectic C LC monomer droplets. Hedgehog defects (A) and tilted Maltese crosses (B) are observed between crossed polarizers. Scale bar is 5 μm . (C) Schematic drawing of the droplet with tilted LCs in the concentric aligned smectic layers. A black Maltese cross is drawn at the position where the LCs are orientated parallel to the polarizers (crossed arrows).

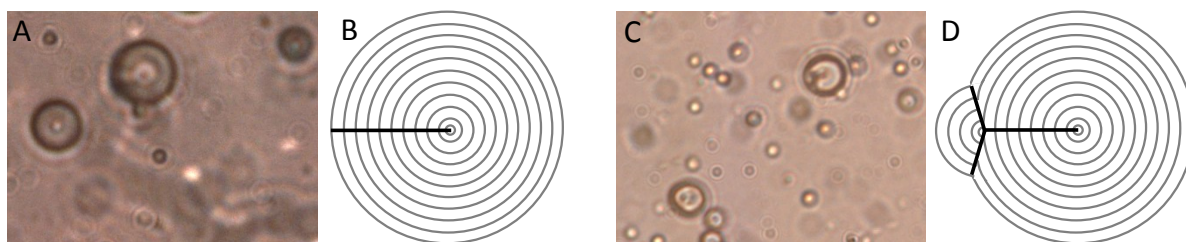


Fig. S7 (A) Microscopy images of smectic C monomer droplets and schematic drawing of the smectic layers within the droplets. Sometimes, in the absence of polarizers optical microscopy images reveal line defects in the larger droplets with droplet sizes of approximately $10\ \mu\text{m}$. (B) It is anticipated that these line defects also occur in the smaller droplets but are difficult to observe due to the limitations of optical microscopy. Moreover, for observations the line should be orientated in a perpendicular fashion with respect to the optical path. When cooled further down the shape of the smectic C droplets change considerably. An additional bulge is formed starting at the disclination line at the droplet surface. The interface between both segments and disclination line are clearly visible (C). An increasing tilt of the LCs results in an increasing surface tension of the droplet. The spherical droplet shape becomes metastable and a distortion means a transition of the system to a stable state, resulting in an equilibrium state with an energetically preferred dumbbell shape (D).

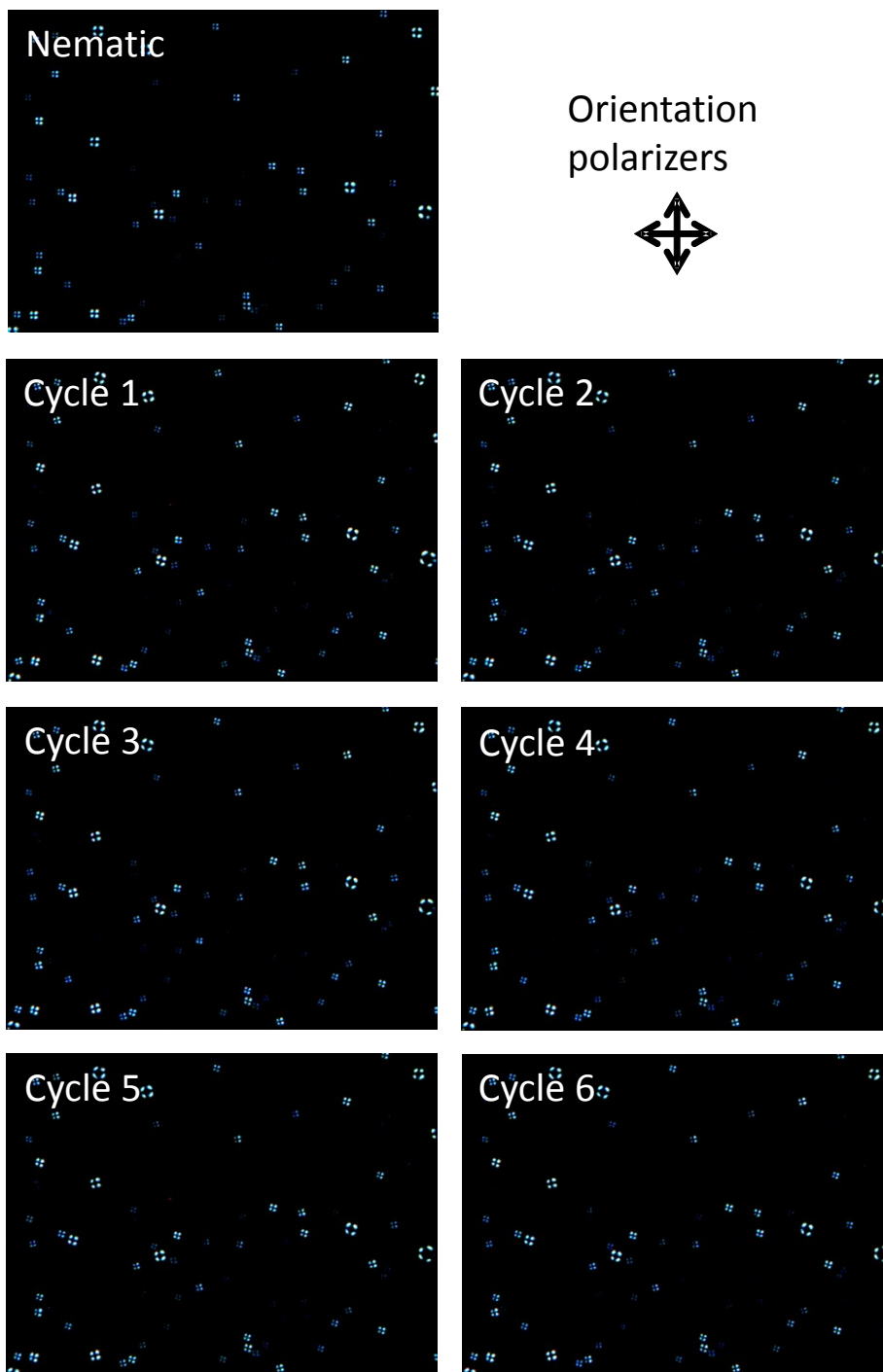


Figure S8. Polarized optical microscopy images of monomer mixture showing the symmetry breaking. Straight Maltese crosses are observed in the nematic phase (70 °C). Upon cooling (60 °C), the LCs start to tilt resulting in tilted crosses. For most droplets, a smooth tilt movement was observed, but sometimes the cross wobbles before it tilts. Six heating – cooling cycles were performed.

S4 Characterization of the polymer particles

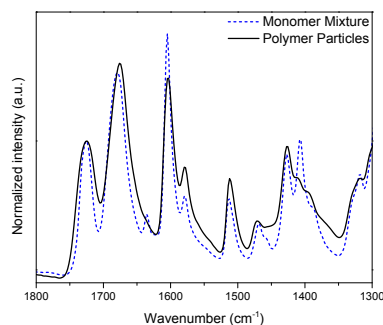


Fig. S9 FTIR spectra of the nOBA-C6H 90-10 monomer mixture and the polymer particles. The C=C bond from the acrylate moiety at 1620 cm⁻¹ is absent for the polymerized particles.

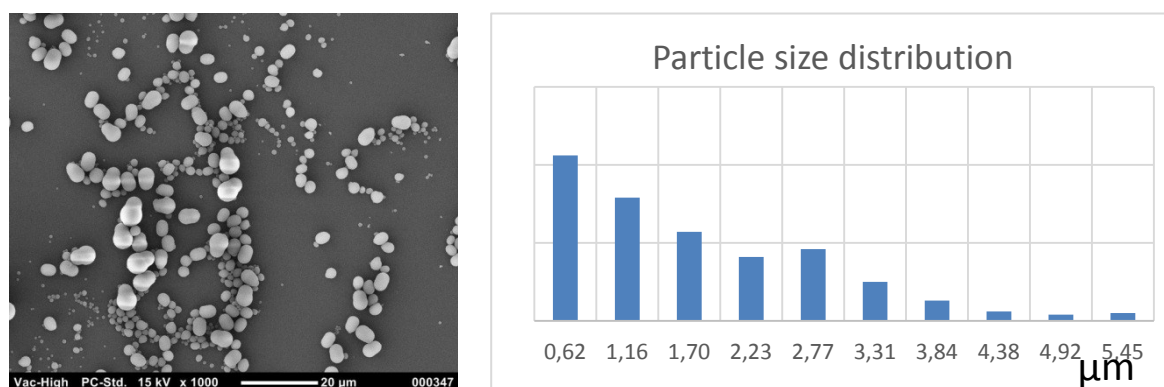


Fig. S10 SEM image revealing a polydisperse particle size with an average of 1.4 μm. Left: SEM picture of the polymer particles. Right: particle size distribution.

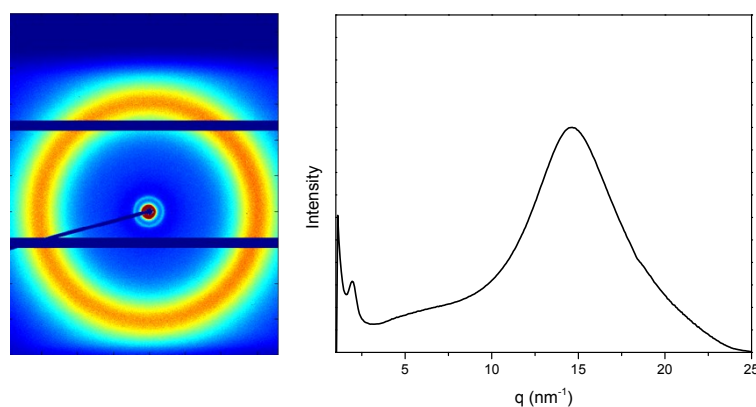


Fig. S11 Left: XRD picture of the polymer particles. Right: 1D profile. The XRD measurements revealed an isotropic powder diffraction pattern. Two distinctive signals were found corresponding to the layer spacing and intermolecular distance. The latter was 0.4 nm. The layer spacing for the smectic C particles was 3.2 nm.

S5 Characterization of the porous polymer particles

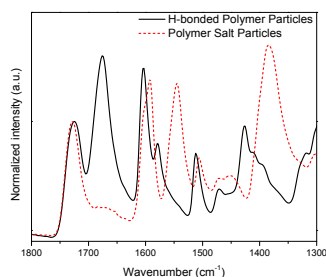


Fig. S12 FTIR spectra of hydrogen bonded polymer particles and the base treated polymer salt particles. The signals at 1675 and 1425 cm⁻¹, corresponding to the carbonyl bond in the hydrogen bonded state and in-plane bending of the O-H bond, respectively, disappeared. Simultaneously, two new vibrations emerged at $\nu_s = 1540$ cm⁻¹ and $\nu_{as} = 1385$ cm⁻¹, and started to appear at pH = 9 to reach a maximum intensity at pH = 9.5. This indicates the formation of a carboxylate salt.

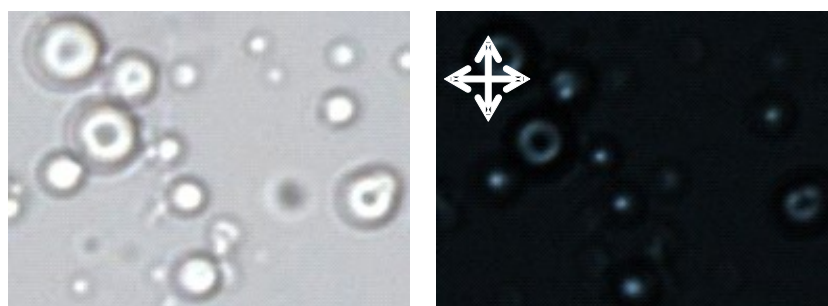


Fig. S13 Left: Microscopy image of nOBA-C6H 90-10 smectic C polymer salt particles showing hedgehog defects and eventually the line defect and interface lines. Right: Between crossed polarizers no alignment can be recognized anymore, due to low birefringence.

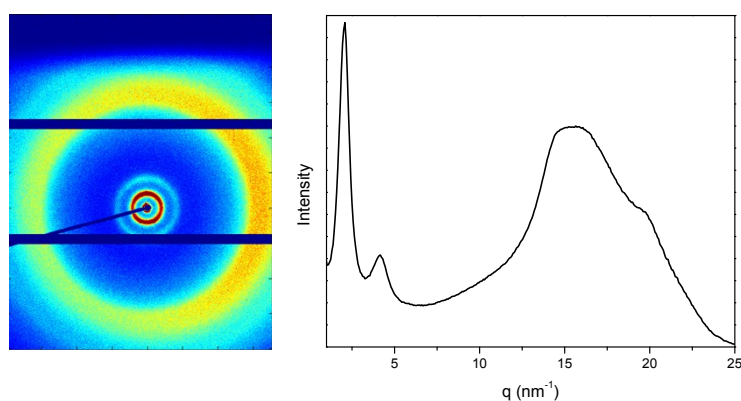


Fig. S14 Left: XRD picture of the porous polymer salt particles. Right: 1D profile. XRD revealed first and second order layer spacing signals corresponding to a spacing of 3.1 nm.

S6 Adsorption characteristics

Adsorption kinetics

Pseudo-second order kinetics can be represented as equation S1. This model was used successfully to describe an adsorption process of methylene blue on the smectic C porous polymer salt particles.

$$\frac{dq}{dt} = k_2(q_e - q_t)^2 \quad (\text{S1})$$

In this equation, k_2 is the rate constant (mol / mol), q_e and q_t are the adsorption at equilibrium and at time t (min), respectively. After integration, reformulation and linearization the equation equals Equation S2.

$$\frac{t}{q_t} = \frac{1}{k_2 q_e^2} + \frac{1}{q_e} t \quad (\text{S2})$$

When $\frac{t}{q_t}$ is plotted against t , the line should be straight and the slope will equal $\frac{1}{q_e}$ and

the intercept will equal $\frac{1}{k_2 q_e^2}$. Thus, $k_2 = \frac{\text{slope}^2}{\text{intercept}}$ and $q_e = \frac{1}{\text{slope}}$

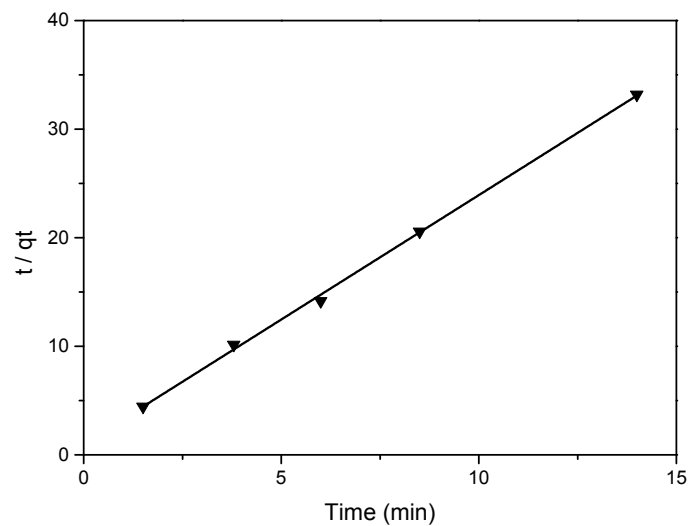


Fig. S15 Pseudo second order kinetics of MB in nOBA-C6H 90-10 smectic C porous polymer salt particles.

Selective adsorption

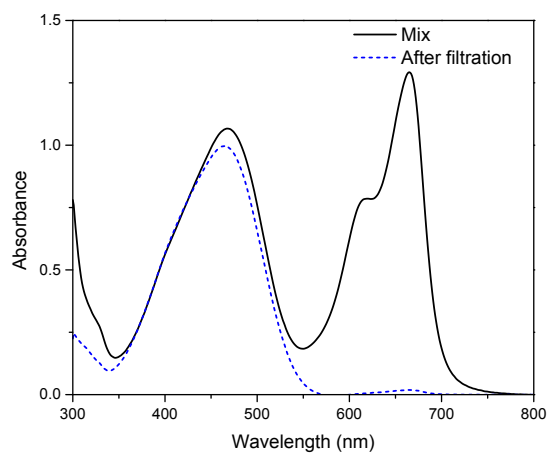


Fig. S16 Selective adsorption and filtration of MB filled particles from a MO – MB dye mixture. UV-vis spectrum of the solutions showing the absence of MB absorbance after filtration.

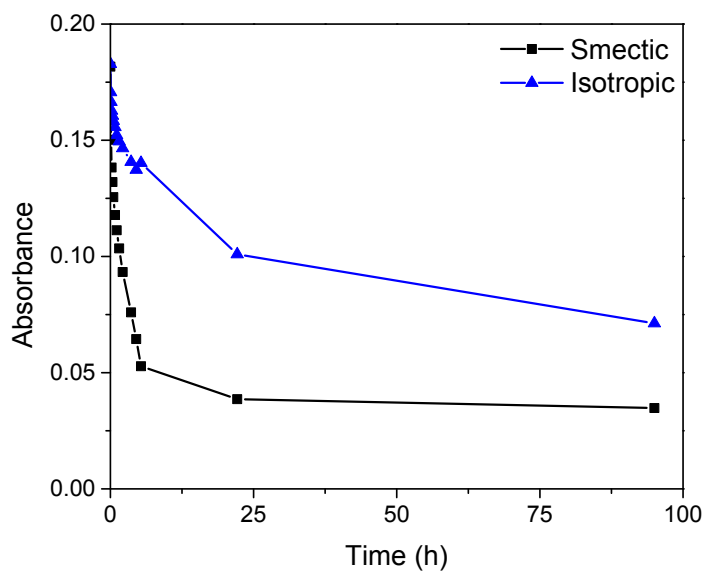


Fig. S17. Dye adsorption of polymer films of similar size polymerized in the smectic and isotropic phase.